Development 139, 2405-2415 (2012) doi:10.1242/dev.078667

Novel mechanisms of early upper and lower urinary tract patterning regulated by RetY1015 docking tyrosine in mice

Masato Hoshi[1], Ekatherina Batourina[2], Cathy Mendelsohn[2] and Sanjay Jain[1,3,*]

SUMMARY

Mutations in the receptor tyrosine kinase *RET* are associated with congenital anomalies of kidneys or urinary tract (CAKUT). RET tyrosine Y1015 is the docking site for PLCγ, a major regulator of RET signaling. Abrogating signaling via Y1015 causes CAKUT that are markedly different than renal agenesis in Ret-null or RetY1062F mutant mice. We performed analysis of Y1015F mutant upper and lower urinary tracts in mice to delineate its molecular and developmental roles during early urinary tract formation. We found that the degeneration of the common nephric ducts (CND), the caudal-most Wolffian duct (WD) segment, depends on Y1015 signals. The CNDs in Y1015F mutants persist owing to increased proliferation and reduced apoptosis, and showed abundance of phospho-ERK-positive cells. In the upper urinary tract, the Y1015 signals are required for proper patterning of the mesonephros and metanephros. Timely regression of mesonephric mesenchyme and proper demarcation of mesonephric and metanephric mesenchyme from the WD depends on RetY1015 signaling. We show that the mechanism of de novo ectopic budding is via increased ERK activity due to abnormal mesenchymal GDNF expression. Although reduction in GDNF dosage improved CAKUT it did not affect delayed mesenchyme regression. Experiments using whole-mount immunofluorescence confocal microscopy and explants cultures of early embryos with ERK-specific inhibitors suggest an imbalance between increased proliferation, decreased apoptosis and increased ERK activity as a mechanism for WD defects in RetY1015F mice. Our work demonstrates novel inhibitory roles of RetY1015 and provides a possible mechanistic explanation for some of the confounding broad range phenotypes in individuals with CAKUT.

KEY WORDS: Ret, CAKUT, Kidney, Ureter development

INTRODUCTION

Urinary tract (UT) development is a complex process that depends on reciprocal interactions between epithelia and surrounding mesenchyme, and timely union, positioning and growth of structures of different embryological origins. Aberrations in a number of steps can result in congenital anomalies of kidney and/or lower urinary tract (CAKUT), the most common cause of renal failure in children (Pope et al., 1999). CAKUT encompass a wide spectrum of upper and lower UT phenotypes, including renal agenesis, hypoplasia, dysplasia, hydronephrosis, ectopic kidneys, mega-ureter, duplication, ureterovesicle junction obstruction, ureterocele and reflux that can occur in isolation or as multiple anomalies in humans and mice. Mutations in many genes have been identified that lead to CAKUT and different mutations in the same gene have also been reported to produce different CAKUT. Delineating genetic and cellular pathways gone awry that lead to these pleiotropic defects is crucial for providing insights into prevention, diagnosis, counseling and management of CAKUT.

In mice the primary connection between the upper and lower UT is established by embryonic (E) day 9.5 (E9.5), when the Wolffian ducts (WDs), paired epithelial tubes in the intermediate mesoderm, insert into the primitive bladder. Cellular rearrangements, proliferation and apoptosis of the WD and its derivatives are crucial for morphogenesis of the UT. During development, three successive kidneys form from the WD in a rostrocaudal manner: the pronephros, mesonephros and the metanephros (Saxen, 1987). The pronephros sprouts from the anterior WD at E8.5, degenerating by E9.5 (Dressler, 2006), when the mesonephros begins to form. The mesonephros consists of the WD and a linear array of mesonephric mesenchyme (MesM). Only the cranial MesM is connected to the WD and differentiates into mesonephric tubules (MesT). During sexual differentiation, the mesonephros degenerates in females. In males, the MesT becomes part of the epididymis and the WD differentiates into vas deferens and seminal vesicles.

The metanephros begins to form from the ureteric bud (UB), an epithelial tube that sprouts from the caudal WD at E10.5 (Dressler, 2006). The distal region of the UB elongates and invades kidney mesenchyme (MetM) by E11.5 and undergoes successive rounds of branching morphogenesis to form the renal collecting duct system. Disruption of UB formation or abnormal sprouting can result in renal agenesis, hypoplasia, dysplasia, duplication, cysts and lower urinary tract defects.

Proper connections between the ureter and the bladder depend on primary connections between the WD and primitive bladder, which occur at E9.5, and ureter maturation, which occurs between E11.5 and E14.5 (Batourina et al., 2002; Batourina et al., 2005; Uetani et al., 2009). Initially, the UB is connected indirectly to the primitive bladder via the caudal WD segment, the common nephric duct (CND). These processes depend on migration, proliferation and apoptosis of the WD and its derivatives. Delay or defects in WD insertion into the primitive bladder, UB formation or ureter maturation can result in abnormal connections between the ureters and bladder, and hence lower UT defects.

[1]Department of Internal Medicine (Renal division), Washington University School of Medicine, St Louis, MO 63110, USA. [2]Departments of Urology, Genetics, and Development and Pathology, Columbia University, New York, NY 10032, USA. [3]Departments of Pathology and Immunology, Washington University School of Medicine, St Louis, MO 63110, USA.

*Author for correspondence (sjain22@wustl.edu)

Accepted 27 April 2012

RET, a transmembrane receptor tyrosine kinase (RTK), regulates the development of many organ systems and its aberrant signaling produces phenotypes in mice that are reminiscent of human diseases such as Hirschsprung disease, CAKUT and MEN2 hereditary cancer syndromes (Amiel and Lyonnet, 2001; Amiel et al., 2008; Jain, 2009; Moore, 2006; Ponder and Smith, 1996; Prato et al., 2009; Skinner et al., 2008). In the urinary system, complete loss or misexpression of Ret results in bilateral renal agenesis, dysplasia, defective insertion of the WD into cloaca and defective ureter maturation (Batourina et al., 2002; Chia et al., 2011; Jain et al., 2006b; Jain et al., 2010; Murawski and Gupta, 2008; Schuchardt et al., 1994; Shakya et al., 2005; Uetani et al., 2009). RET signaling in kidneys is activated by the formation of a receptor complex with glial cell line-derived neurotrophic factor (GDNF) and GFRα1 co-receptor (Jain, 2009). Activation of RET results in phosphorylation of major docking tyrosine (Y) residues in the cytoplasmic domain of RET that interact with cellular adaptors to activate key signaling cascades such as PLCγ, SRC, PI3K and MAPK. These regulate cellular processes such as proliferation, migration, differentiation, survival and self-renewal to ensure normal development. In our previous studies, we generated individual Ret-docking tyrosine mutant mice and discovered that RetY1015 (docking site for PLCγ) and RetY1062 (which activates the PI3K/MAPK pathway through adaptors such as Shc) have distinct roles in the UT and the autonomic nervous systems (Jain et al., 2006a; Jain et al., 2010). *RetY1015F* mutants display spectrum of CAKUT-like defects, including supernumerary ureters, mega-ureters and dysplasia, as well as abnormally positioned gonads and failure of gonadal ducts to separate from the ureter. *RetY1062F* mutants show rudimentary kidneys, hypoplasia or agenesis (Jain et al., 2006a; Jain et al., 2004; Jijiwa et al., 2004; Wong et al., 2005). The molecular, cellular and developmental basis for disparate defects encompassing a wide range of CAKUT in these mutants is not known.

We performed early developmental, molecular and cellular analysis of *RetY1015F* UTs and found that RetY1015 signaling regulates multiple aspects of WD development, maturation, connection to the bladder and the fate of surrounding mesenchyme even before definitive kidney is formed. These studies illuminate on mechanisms of RTK-mediated specificity and portray a novel inhibitory roles of RetY1015, before metanephric kidney develops, that are crucial to ensure normal urinary system patterning and prevention of renal malformations.

MATERIALS AND METHODS

Animals

Institution approved protocols were followed for all animal studies. For timed pregnancies, the day of the copulatory plug was defined as embryonic day 0.5 (E0.5). $Ret^{EGFP/+}$ reporter mice expressing EGFP from the *Ret* locus were generated by breeding *Ret floxEGFP* mice (Jain et al., 2006a) with *β-actin Cre* mice (Meyers et al., 1998). *Cre* was removed by subsequent breeding with wild-type mice (supplementary material Fig. S1). Genotyping was performed using PCR with primers P6855 (Jain et al., 2006b) and P8428 (Jain et al., 2006b). Mice used for experiments were on a mixed background (*129/SvJ:C57BL/6*). *Gdnf*-null and *Ret*Y1015F tyrosine mutant mice were described previously (Jain et al., 2006a; Moore et al., 1996). For *RetY1015F* mutant analysis we used *Ret9Y1015F* or *Ret51Y1015F* mice as they both have similar kidney phenotypes and are referred to as *RetY1015F* in this manuscript. To facilitate visualization of Ret-expressing cells by virtue of EGFP expression, *Y1015F* hemizygous mice ($Ret^{Y1015F/+}$) were bred with *RetEGFP* hemizygous ($Ret^{EGFP/+}$) mice. Urinary tract defects are identical in mice expressing only single mutant (*Y1015F*) allele with *Ret-EGFP* reporter allele ($Ret^{Y1015F/EGFP}$), or double *Y1015F* homozygous alleles ($Ret^{Y1015F/Y1015F}$). Slit2-null mice were obtained from MMRCC (strain #030405-MU).

Morphological and immunofluorescence analysis

Mouse tissues were harvested at the indicated ages, fixed in 4% paraformaldehyde (PFA) and processed as previously described (Jain et al., 2004). Routine histological assessment was carried out on Hematoxylin and Eosin-stained tissue sections. Immunostaining of whole organs and tissue sections was as previously described (Jain et al., 2006a; Jain et al., 2010). The antibodies used were: anti-Pax2 (Covance, 1:100), anti-GFP (Aves, 1:200), anti-mouse E-cadherin (R&D, 1:50) and anti-phospho ERK1/2 and Histone H3 (Cell Signaling, 1:100). Secondary antibodies were Alexa-488-conjugated anti-chicken IgY, Cy3-conjugated anti-goat or anti-rabbit IgG, Cy5-conjugated anti-goat IgG (Jackson ImmunoResearch, 1:200), and Alexa488-conjugated anti-rabbit IgG (Molecular Probes, Invitrogen, 1:200).

Organ culture

Whole-mount cultures of UT or metanephros alone from mutant and control embryos were grown in serum-free defined media on transwell filters (0.4 μm) in six-well plates (Rogers et al., 1991). E10 half GU cultures (each half cultured separately) for determining role of ERK signaling were grown in presence of the ERK inhibitor U0126 (10 μM, Sigma) or with DMSO (vehicle). These cultures were propagated using an environmentally controlled (37°C, 5% CO_2) chamber for the times indicated in the text.

Microscopy

Whole-mount specimens were visualized with a fluorescence stereomicroscope and tissue sections on a compound upright microscope; images were captured as previously reported (Jain et al., 2010). Time-lapse microscopy was performed on a motorized inverted microscope (Nikon TE2000, Nikon Instruments, Melville, NY) and the images were captured by HQ2 (Photometrics, Tucson, AZ) camera. Confocal microscopy analysis with *z*-stacking was performed with Nikon C-1 confocal system. The analysis and 3D reconstruction were performed by Nikon Elements software (Nikon). The images were processed and analyzed with Metamorph (Molecular Devices), Nikon Elements (Nikon) or Adobe Photoshop (Adobe) software.

Whole-mount in situ hybridization

Fixed embryos were pre-treated in DEPC-treated PBS containing 0.3% Triton X-100, 7.5 μg/ml proteinase K for 15 minutes at room temperature followed by post-fixation with 4% PFA containing 0.2% glutaraldehyde for 30 minutes at room temperature. After washing, specimens were prehybridized in hybridization solution [50% formamide, 5×SSC (pH 4.5), 0.5% CHAPS, 0.1% Tween 20, 5 mM EDTA, 50 μg/ml yeast tRNA, 50 μg/ml heparin] for 1 hour followed by overnight incubation in hybridization solution containing the probe (2 μg/ml) at 65°C. After washing [0.1×SSC (pH 4.5), 0.5% CHAPS, 0.1% Tween 20] at 65°C and RNase treatment, specimens were incubated with alkaline phosphatase-conjugated anti-DIG antibody (Roche, 1:2000) and positive signals were visualized using NBT/BCIP (Roche). *Gdnf* antisense RNA in situ probe was made from E14.5 embryonic head cDNA library by cloning a 2 kb fragment of Gdnf cDNA (NM010275; nt121-2068) into pBluescript KS (+), and T3 polymerase was used for antisense transcription on *Bam*HI-digested plasmid. For the *Spry1* probe, a 2 kb fragment of Spry1 cDNA (NM011896; nucleotides 99-2422, lacking exon 2) was cloned as above and T3 transcription was carried out on *Eco*RI-digested plasmid. Plasmid for *Slit2* probe was kindly provided by Dr Gail Martin, and T7 was used for anti-sense transcription.

X-gal and TUNEL staining

Previously reported procedures for X-gal (Enomoto et al., 1998) and TUNEL (Jain et al., 2004) staining were used on fixed tissue. TUNEL-positive cells were visualized with streptavidin-conjugated DyLight-647 or -488 (Jackson ImmunoResearch, 1:200).

Quantitative analysis

For determining differences between control and mutant animals, the stained sections were visualized using confocal microscopy and *z*-stack images were constructed through the entire WD or CND and all individual cells in the given region were counted. Statistical significance was determined with Student's *t*-test unless otherwise specified. The sample size was three or more for each genotype used.

RESULTS

GU defects in *RetY1015F* mutant mice manifest during early WD patterning

To delineate the developmental mechanisms by which mice with deficient RetY1015 (PLCγ adaptor site) signaling develop CAKUT phenotypes, we performed developmental analysis of GU system in mouse embryos with *RetY1015F* mutation. To readily identify Ret-expressing structures and associated pathologies, we generated a mouse line that expresses enhanced green fluorescent protein (EGFP) from *Ret* locus (*RetEGFP*) (supplementary material Fig. S1). *RetY1015F* mice were bred with *RetEGFP* reporter mice to obtain mice that only express mutant *RetY1015F* ($Ret^{Y1015F/EGFP}$) allele. Ret-hemizygous littermates from the breeding were used as controls ($Ret^{EGFP/+}$).

Analysis of *RetY1015F* mutants at E9.5 revealed similar anteroposterior development as in controls (Fig. 1A). At E10.5, the controls show UB initiation at the posterior WD, visible as a thickened domain. In Y1015F mutants, however, segments of abnormal swellings with high Ret expression were seen in the anterior WD and the posterior UB-budding domain was markedly increased (Fig. 1A). At E11.5, these swellings in Y1015F mutants were more pronounced and readily apparent as ectopic UBs throughout the anterior WD, and at the level of the putative kidney, neither of which was observed in controls. In the primary UB budding domain, multiple outgrowths with high EGFP signal were evident in *RetY1015F* mutants compared with a single UB from each distal WD in controls. Common nephric duct (CND) appeared elongated and persisted in *RetY1015F* mutants (Fig. 1A; see later). Examination of the GU tracts at later time points revealed more severe phenotypes, including multiplexed, dysplastic kidneys, gonadal dysgenesis, multiple ureters and obstruction.

To better understand the fate of extraneous UBs, their role in producing multiplexed metanephroi and impact of the Y1015F mutation on lower tract formation, we performed time-lapse imaging of whole GU cultures in control (Fig. 1B, top; supplementary material Movie S1) and *RetY1015F* (Fig. 1B, bottom; supplementary material Movie S2) mutant mice beginning at E11.5. We noted de novo UBs were formed from the anterior WD of *RetY1015F* mutants and some of the caudal mesonephric UBs fused with metanephros and led to multiplexed, abnormally branching kidneys. The time-lapse images and movies also showed that the CND of *RetY1015F* mutant mice did not regress as they continued to exhibit high EGFP expression.

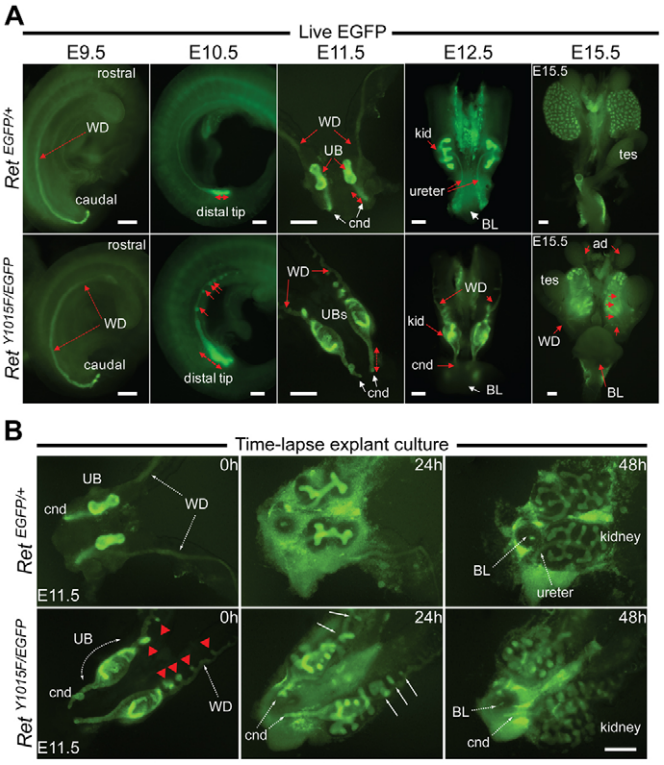

Fig. 1. Upper and lower urinary tract anomalies in *RetY1015F* mice occur early during Wolffian duct morphogenesis. (**A**) At E9.5, Ret expression pattern (green EGFP signal) indicates that Wolffian ducts (WD) in control (top, $Ret^{EGFP/+}$) and mutant *RetY1015F* (bottom, $Ret^{Y1015F/EGFP}$) mice develop normally. The earliest abnormalities in the *RetY1015F* WDs are seen at E10.5 as abnormal bulges (red arrows) throughout and marked expansion of the distal WD (dashed double-headed arrow). At later time points (E11.5, E12.5 and E15.5), these transform into multiple ectopic ureteric buds (UBs), abnormal branching, gonadal mislocation and separation failure of ureter from WD. At E11.5, common nephric ducts (CND) in *RetY1015F* mice are elongated and persist (supplementary material Movie 2). Scale bars: 250 μm. cnd, common nephric duct; kid, metanephric kidney; BL, bladder; ad, adrenal gland; tes, testis. (**B**) Time-lapse microscopy images of whole GU tract culture of control (supplementary material Movie 1) or mutant (supplementary material Movie 2) animals at the indicated time points beginning at E11.5. In *RetY1015F*, the ectopic buds are new outgrowths from the anterior WD, and UBs invading the metanephric mesenchyme branch abnormally (arrows in the middle panel). Some mesonephric ectopic buds merge with the metanephric kidney, resulting in multi-lobed structures. The CND persists in *RetY1015F* mutants compared with control littermates (supplementary material Movie 2). Scale bar: 250 μm.

RetY1015 mediates timely regression of caudal mesonephros

Reciprocal interactions between the Ret-expressing UB and the surrounding MetM are crucial for kidney development. How the interactions between WD and the mesonephric mesenchyme (MesM) impact the development of the kidney are less defined. We hypothesized that abnormal interaction between the MesM and *RetY1015F* mutant WDs plays a role in ectopic UBs. To test this, we first examined detailed normal process of mesonephros development beginning at E8.5 using whole-mount Pax2 immunostaining (supplementary material Fig. S2A). This analysis showed that MesM degeneration begins at about E10.5 extending in a caudal to cranial fashion. By E11.5 ,caudal MesM is degenerated completely and only the cranial-most MesT that are connected to the WD persist as epididymis in males (Smith and Mackay, 1991). In the blastema, which forms the metanephric kidney, strong Pax2-staining was evident as expected (Brophy et al., 2001). In *RetY1015F* mutants, however, Pax2-positive MesM condensations persisted all along the WD compared with controls (Fig. 2). This anteroposterior mesonephros patterning defect shows that RetY1015-mediated WD-derived signals (as Ret is only expressed in the WD) regulate MesM degeneration.

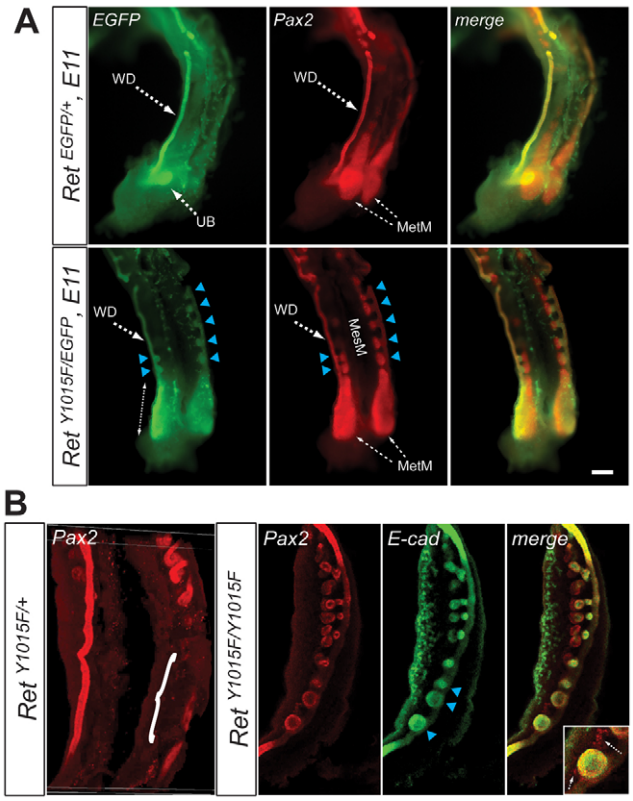

Fig. 2. Persistent caudal mesonephros in *RetY1015F* mice. (**A**) Double immunostaining with Pax2 and GFP antibodies shows persistence of linear aggregates of mesonephric mesenchyme in *RetY1015F* mutants (arrowheads) at E11. Controls (RetEGFP/+) show almost complete degeneration of these structures. (**B**) Different views from confocal microscopy images confirm the persistence of MesM (Pax2-positive red spherical structures) and its invasion by the ectopic UBs (green, E-cadherin immunostaining; arrowheads) in *RetY1015F* homozygous mice. The merged image clearly shows the red Pax2-positive cells surrounding the green UB (inset, arrows). In controls (*Ret*$^{Y1015F/+}$), Pax2 immunostaining shows labeling of only the cranial MesT and absence of caudal MesM (white bracket). Two different views are shown to highlight the WD and the mesonephros. Scale bar: 200 μm.

Reduced Gdnf gene dose ameliorates ectopic UB phenotype but not the persistent MesM in *RetY1015F* mutants

The persistence of MesM in *RetY1015F* mice and Pax2 expression further supported the idea that the ectopic UBs formed in response to tropic factors from the MesM, including GDNF (Brophy et al., 2001; Grote et al., 2008; Maeshima et al., 2007; Sainio et al., 1997; Shakya et al., 2005). Whole-mount *Gdnf* in situ hybridization of *RetY1015F* mice and X-gal staining of *RetY1015F:Gdnf β-gal* mice confirmed *Gdnf* misexpression in the MesM of *RetY1015F* mice at E11.5 (supplementary material Fig. S2B). To determine conclusively whether ectopic Gdnf expression in MesM indeed contributes to supernumerary UBs and the CAKUT phenotypes, we used a genetic approach and reduced *Gdnf* gene dose in *RetY1015F* mice. Analysis of the urinary tracts in *Gdnf-Het:RetY1015F* mice after birth revealed markedly decreased severity of the CAKUT phenotypes and a subset of animals even showed normal urinary tracts (two out of 11, Fig. 3A,B). To examine the effects of *Gdnf* reduction during early WD development, we performed whole-mount Pax2 and E-cadherin immunohistochemistry in *RetY1015F* and *Gdnf-Het:RetY1015F* mutants. The analysis revealed that *Gdnf* haploinsufficiency in *RetY1015F* mice led to fewer ectopic buds and a reduction in abnormal distal expansion of the WD, compared with *RetY1015F* mice with normal *Gdnf* dose (Fig. 3C).

Interestingly, despite the improvement in CAKUT in *Gdnf-Het:RetY1015F* mice, caudal MesM did not regress as Pax2 positivity was still detected in MesM (Fig. 3C). This suggests that the fate of caudal MesM is dependent on RetY1015 signals from WD and not on ectopic UBs or Gdnf. To affirm this conclusively, we completely eliminated *Gdnf* in *RetY1015F* mutants (double homozygous) and analyzed urinary tract development. These experiments revealed complete lack of UB formation (ectopic or normal) in three out of three double homozygous mutant mice, further confirming extraneous Gdnf as a mechanism of ectopic UBs in these mice (Fig. 3D). However, high *Gdnf* promoter activity and Pax2 expression persisted as linear aggregates along the WD (two out of three double homozygous mice) in *Gdnf-Hom:RetY1015F* double homozygous mice. Sustained and high *Gdnf* expression in the double homozygous urinary tracts was also confirmed by whole-mount *Gdnf* in situ hybridization (Fig. 3E). These results suggest that RetY1015 signaling in the WD provides inhibitory cues to promote regression of the caudal MesM. Failure of this results in extraneous Pax2 and Gdnf expression, which provides tropic support for ectopic bud formation.

RetY1015 signals specify the boundary between the mesenchyme and Wolffian duct

The persistence of MesM in *RetY1015F* mice prompted us to examine whether there were abnormalities in MesM and MetM in relation to WD that may also contribute to abnormal budding. We first compared MesM in controls, *RetY1015F* and Ret nulls at E10.5, a time-point before mesonephros degeneration and UB branching occurs. Whole-mount confocal microscopy with 3D reconstruction using kidney epithelial and mesenchymal markers (E-cadherin and Pax2) showed a well-developed MesM that is clearly separated from the WD in controls and *Ret*-null mice (Fig. 4A). By contrast, *RetY1015F* mutant MesM was malpositioned and abutting on WD with little or no demarcation. The close proximity of MesM to the anterior WD probably further contributes to providing strong tropism for ectopic UBs from WD.

We next examined whether there were positional abnormalities in MetM in *RetY1015F* mutant mice at E11, a time-point when the UB has just invaded into MetM (Fig. 4B). E11 control kidneys showed a well developed, distinct oval-shaped MetM clearly separated from the WD by a single UB stalk (Fig. 4B, left). In *RetY1015F* mutants, several broad UB bulges were apparent from the abnormal distal UB budding domain in WD. MetM was abnormally juxtaposed, overlaying on the distal WD without any intervening space (Fig. 4B, middle). Thus, altered distal WD-MetM topology sets a precedent for MetM to provide strong UB stimulating signals over a widely extended primary UB domain in the mutant distal WD. It is possible that the abnormal MetM positioning on the WD in Y1015F UTs is due to extra UBs. To test this hypothesis, we assessed WD-MetM relationships in *Slit2*-null mice (Grieshammer et al., 2004) that have similar CAKUT as RetY1015F, including caudal ectopic UBs (Fig. 4B, right). We observed that the morphology of WD, UB budding and MetM in *Slit2*-null mice was markedly different from RetY1015F and not just secondary to the increase in UBs (Fig. 4B,C). These results together suggest that normal RetY1015 function is necessary to maintain proper demarcation between the MesM/MetM and WD.

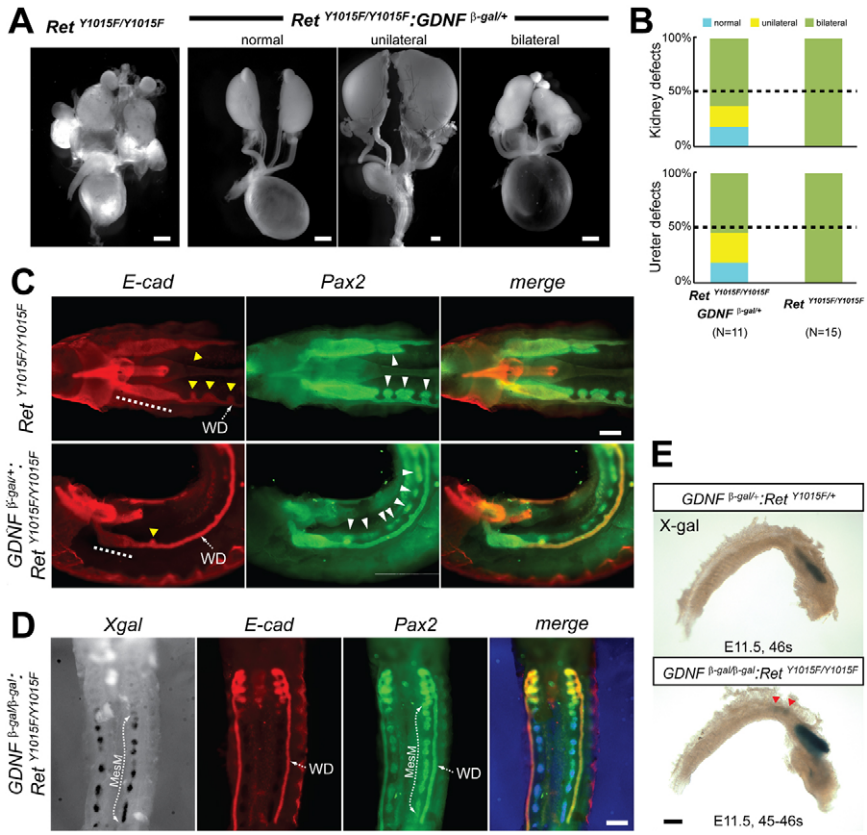

Fig. 3. Reduced GDNF improves CAKUT but not the persistent MesM in *RetY1015F* mice. (**A**) Reduced *Gdnf* gene dose improves CAKUT phenotypes in *RetY1015F:Gdnf*-het mice. Compared with multiple bilateral CAKUT in all *RetY1015F* mice, compound *RetY1015F:Gdnf-het* mice show milder kidney, ureter and gonadal defects, suggesting that extra UBs, gonadal mislocalization and mega-ureters are due to increased GDNF-mediated signals. Representative gross images are shown to highlight spectrum of defects in the compound het animals. (**B**) Gross unilateral or bilateral defects in the ureter (dilated) or kidney (multiplexed) in the indicated mice. (**C**) Whole-mount Pax2/E-cadherin double immunostaining illustrates that *Gdnf* haploinsufficency in E11 *RetY1015F* embryos reduces ectopic UBs (yellow arrowheads), decreases distal expansion of WD (broken line), but shows persistence of MesM (white arrowheads). (**D**) Images of the anterior E11 WDs (red E-cadherin staining) of *RetY1015F* embryos with complete *Gdnf* deletion show no ectopic UBs. However, presence of Pax2 positivity (green) and *Gdnf*-driven X-gal staining (blue) in MesM in the double mutants indicates that RetY1015 signals regulate caudal mesonephros degeneration independently of GDNF. (**E**) Whole-mount X-gal staining (blue) at E11.5 further confirms persistent MesM (red arrowheads) in *Gdnf-null:RetY1015F* mice. Scale bars: 1 mm in A; 200 μm in C,D; 250 μm in E.

RetY1015 regulates apoptosis in MesM and UB budding domain

We performed TUNEL analysis to determine whether persistence of MesM and the abnormally expanded Ret-expressing region in the distal WD in *RetY1015F* mutant mice were due to defects in apoptosis. Confocal images of whole-mount TUNEL staining at E10.5 revealed reduced apoptosis in the caudal MesM of *RetY1015F* mutant mice compared with controls (Fig. 5A). At E11.5, whole-mount TUNEL staining in control animals revealed TUNEL-positive cells all along the WD, except that the very distal Ret-positive UB budding domain was apoptosis free (Fig. 5B). By comparison, in *RetY1015F* WDs, the distal apoptosis-free zone was significantly longer and overlapped with the high Ret-expressing region. We did not see any significant differences in apoptosis in rostral regions of WDs in the mutants and controls.

Phospho-ERK activity is increased in *RetY1015F* mesonephros

ERK signaling promotes cell survival and is one of the main downstream signaling pathways activated by receptor tyrosine kinases (RTK), including Ret (Sebolt-Leopold and Herrera, 2004). Reduced apoptosis in *RetY1015F* urinary tracts prompted us to examine further whether this was due to increased phospho-Erk (pERK) activity. Using whole-mount pERK and E-cadherin double immunostaining and confocal microscopy, we found that *RetY1015F* mutant mice had marked increase in pERK staining in both WD and the surrounding mesenchyme compared with controls or *Ret*-null UTs (Fig. 5C,D). We did not find any difference in pAKT immunostaining between control and mutant UTs (supplementary material Fig. S3).

Slit2 and *Spry1* expression are not affected in *RetY1015F* mutant mice

Slit2 and *Spry1* loss results in CAKUT phenotypes that are similar to those in *RetY1015F* mice (Basson et al., 2005; Grieshammer et al., 2004). Spry1 inhibits MAPK activity, its expression can be regulated by RTK signaling and it interacts with the Gdnf-RetY1062 pathway (Basson et al., 2005; Kim and Bar-Sagi, 2004; Michos et al., 2010; Rozen et al., 2009; Vainio and Muller, 1997). We performed Spry1 quantitative RT-PCR and whole-mount in situ hybridization on E11.5 UTs in control and *RetY1015F* mice to determine whether loss of Spry1 expression is the reason for the kidney defects in *RetY1015F* mice. The results showed no significant decrease or loss of *Spry1* expression in *RetY1015F* mice (Fig. 5E). We did not detect any changes in *Slit2* expression in *RetY1015F* urinary tracts either (Fig. 5E). These results suggest that the CAKUT phenotype in *RetY1015F* mutants is not due to loss of *Spry1* or *Slit2* expression.

Altered CND fate in *RetY1015F* mice

To determine the mechanisms of enlarged ureters and their failure to separate from WD in *RetY1015F* mice, we next examined the development of uretero-vesicle junction (UVJ). The ability of WDs to successfully reach cloaca and CND degeneration are two crucial steps that determine successful separation of the ureter and the WD, and joining of the ureter with the bladder (Batourina et al., 2002; Batourina et al., 2005; Chia et al., 2011; Uetani et al., 2009). Whole-mount E-cadherin immunostaining and visualization of Ret-EGFP signal at E10.5 indicated that *RetY1015F* WDs were able to reach the cloaca as in controls (Fig. 6A). However, analysis at later time points showed that mutant WDs and ureters failed to separate, as demonstrated by persistent Ret-EGFP signal in the *RetY1015F*

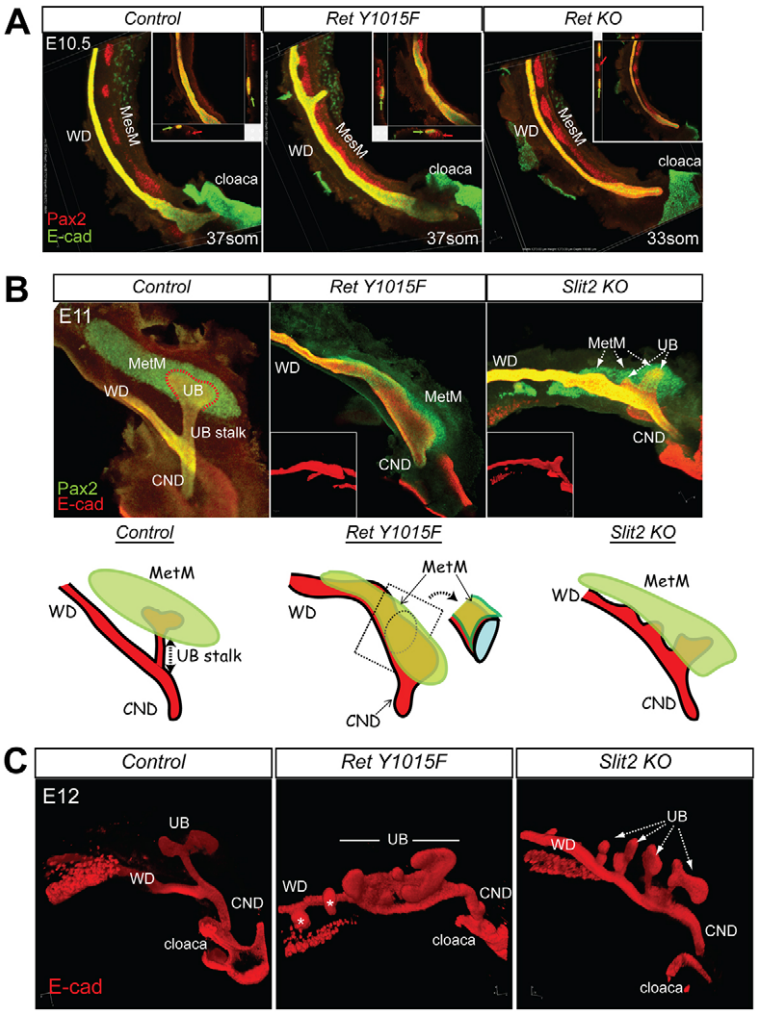

Fig. 4. RetY1015 signaling regulates topological relationship between Wolffian duct and mesonephric and metanephric mesenchymes. (**A**) Mesonephric mesenchyme (MesM) is abnormally positioned next to the Wolffian duct (WD) in *RetY1015F* mice. The images are composite confocal microscopy images of E10.5 control or indicated *Ret* mutants obtained from Pax2 (red), E-cadherin (green) double whole-mount immunofluorescence experiments. In *RetY1015F* mice only, the MesM is not clearly separated from WDs. Insets are 3D cross-sectional renderings of confocal images displayed on two axes clearly depicting the close apposition of MesM (red arrow) and WD (green arrow) in *RetY1015F* compared with the other mice. (**B**) Metanephric mesenchyme (MetM) is malpositioned in *RetY1015F* mutant mice. Confocal images of whole-mount double Pax2-E-cadherin staining at E11 shows that MetM overlays on the extended ureteric bud (UB) budding domain in *RetY1015F* mutant WDs almost enveloping it. By contrast, MetM in controls with single UB or in *Slit2* nulls with multiple UBs are separated by a stalk. Insets show E-cadherin-stained WDs (red), showing marked difference in WD morphology in *RetY1015F* and *Slit2*-null mice at E11. Illustration highlights aberrant MetM-WD topology in *RetY1015F* mutant mice. (**C**) 3D renderings of E12 E-cadherin-stained confocal microscopy images demonstrate markedly abnormal budding owing to malpositioned MetM in *Ret Y1015F* mutant compared with multiple UBs in *Slit2*-null mice. CND, common nephric duct.

mutant CNDs, indicating that they did not degenerate (Fig. 6A; supplementary material Movie S2). Confocal images of whole-mount E-cadherin and EGFP immunostaining at E12.5 further showed a distinct CND on the cloacal surface of *RetY1015F* embryos that extended further than its normal fusion site (Fig. 6A,B). Serial histological sections through embryonic UVJ at E12.5 also confirmed a single CND lumen that is more distally located near the bladder-urethera junction in *RetY1015F* mutants compared with controls with distinct WD and ureter lumens at this stage (Fig. 6B, not shown). Whole-mount TUNEL staining in conjunction with confocal microscopy revealed that persistence of the CND was due to reduction in distal CND apoptosis in *RetY1015F* mice compared with controls at E11.5 and E12.5 (Fig. 6C; supplementary material Fig. S4). At E11.5, the *RetY1015F* mutant CNDs had increased phospho-Histone H3 labeling, indicating increased proliferation (Fig. 6D). Comparison of proliferation at E12.5 between the controls and mutant was difficult as part of the CND normally degenerates in the control. Because Ret-dependent PI3K/MAPK activity is mitogenic and promotes survival, we examined whether increased activity of this pathway in the distal mutant CNDs may explain increased proliferation and survival. We observed significantly increased pERK-positive cells in the mutant CNDs (Fig. 6E). These results suggest that RetY1015 signals regulate precise timing of CND degeneration by modulating ERK activity, proliferation and apoptosis.

Inhibition of MAPK attenuates abnormal budding and distal WD UB budding domain in RetY1015F mice

To further confirm that the mechanism of WD rostral and caudal abnormalities in RetY1015F mutants is due to increased ERK activity, we performed half GU time-lapse cultures of control and mutant mice with a specific MAPK inhibitor (U0126) beginning at E10.0. Phase-contrast and live EGFP images clearly show that MAPK inhibition attenuates mesenchymal Pax2 expression and ectopic budding, and causes distal WD/CND aplasia compared with vehicle-treated controls (Fig. 7).

DISCUSSION

In this study, we determined the fetal origins and molecular and developmental mechanisms of a complex CAKUT phenotype in mice with mutation in key Ret docking tyrosine, Y1015. We generated a new robust Ret-reporter strain (RetEGFP) and used time-lapse microscopy of the entire GU tract to demonstrate that the UT defects occur early in development, before metanephric kidney begins branching morphogenesis. Our results show that Y1015 signals suppress ectopic UBs from the mesonephric WD, regulate the timing of MesM degeneration, establish proper boundaries between the mesenchyme and the WD, and regulate CND degeneration (Fig. 8). Our analysis shows that these

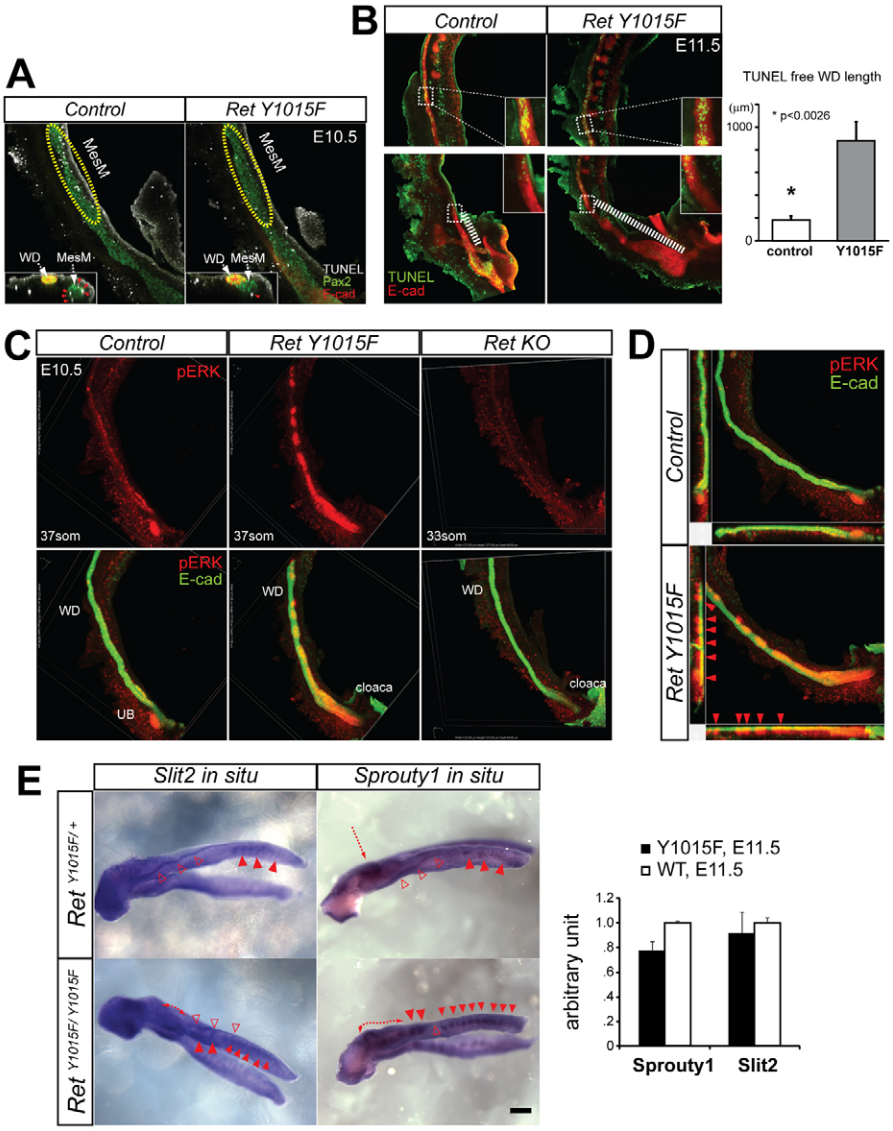

Fig. 5. Reduced apoptosis, increased pERK but no change in Spry1 or Slit2 expression in RetY1015F mesonephros. (**A**) Triple whole-mount confocal immunostaining for TUNEL (white), Pax2 (red) and E-cadherin (green) at E10.5 shows decreased caudal mesonephric mesenchyme (MesM) apoptosis in *RetY1015F* mice. Caudal MesM (yellow outline) in *RetY1015F* exhibits fewer TUNEL-positive cells than control. Inset represents transverse view of 3D reconstructed images (red arrowheads, TUNEL-positive cells in MesM). (**B**) Reduced apoptosis in caudal Wolffian ducts (WDs) of *RetY1015F* urinary tracts (UTs) (bottom panel). 3D reconstructed confocal images of whole-mount TUNEL (green) and E-cadherin (red) double staining in control and *RetY1015F* UTs at E11.5 show increased TUNEL-free region in distal WD in mutants. The insets show enlarged views of the transition of TUNEL-free and TUNEL-positive area. TUNEL staining in rostral WDs appeared similar in controls and RetY1015F mutants (top panel, inset higher magnification). Graph shows quantification of the length of TUNEL-free WD between controls and mutants (three GU tracts from each genotype, mean±s.d., **P*<0.0026; *t*-test). (**C**) Increased pERK in *RetY1015F* WD and MesM. Composite confocal images of the UTs using double whole-mount immunolabeling with pERK (red) and E-cadherin (green) of indicated mice at E10.5. Top row shows increased pERK only in *RetY1015F* compared with controls and *RetKO* mice. Bottom row shows merged images confirming pERK staining in the WD and in the MesM surrounding the WD in *RetY1015F* mice. (**D**) Cross-sectional 3D renderings of confocal images of control and *RetY1015F* mice confirm pERK staining (red arrowheads) next to the double pERK/E-cadherin-labeled WD in *RetY1015F* mice. (**E**) *Spry1* and *Slit2* mRNAs are expressed at similar levels in *RetY1015F* and control mice. Left, whole-mount in situ hybridization (blue staining) shows expression in the WD and ectopic UBs. WD, open red triangles; MesT or MesM, closed triangles; MetM, red arrow or double arrowheads. Right, quantitative RT-PCR shows similar *Spry1* and *Slit2* mRNA levels in control and *RetY1015F* UTs (*n*=2 independent UT RNA pools).

inhibitory roles of RetY1015 are necessary to coordinate precise timing of WD, CND and mesenchymal apoptosis, balancing ERK signaling, UVJ formation and ureter remodeling.

One novel result and insight from our study is the inhibitory role of RetY1015 in modulating cell survival and ERK signaling at multiple stages of WD patterning. Failure of this regulation is one of the mechanisms of ectopic UBs, multiplexed kidneys and ureter abnormalities. In mammals, the caudal mesonephros must regress at a precise time. We showed that RetY1015 regulates this process. RetY1015-mediated inhibitory signals in the WD control the timing of MesM degeneration. These signals in the WD also ensure that the MesM and the MetM are able to maintain a distance from

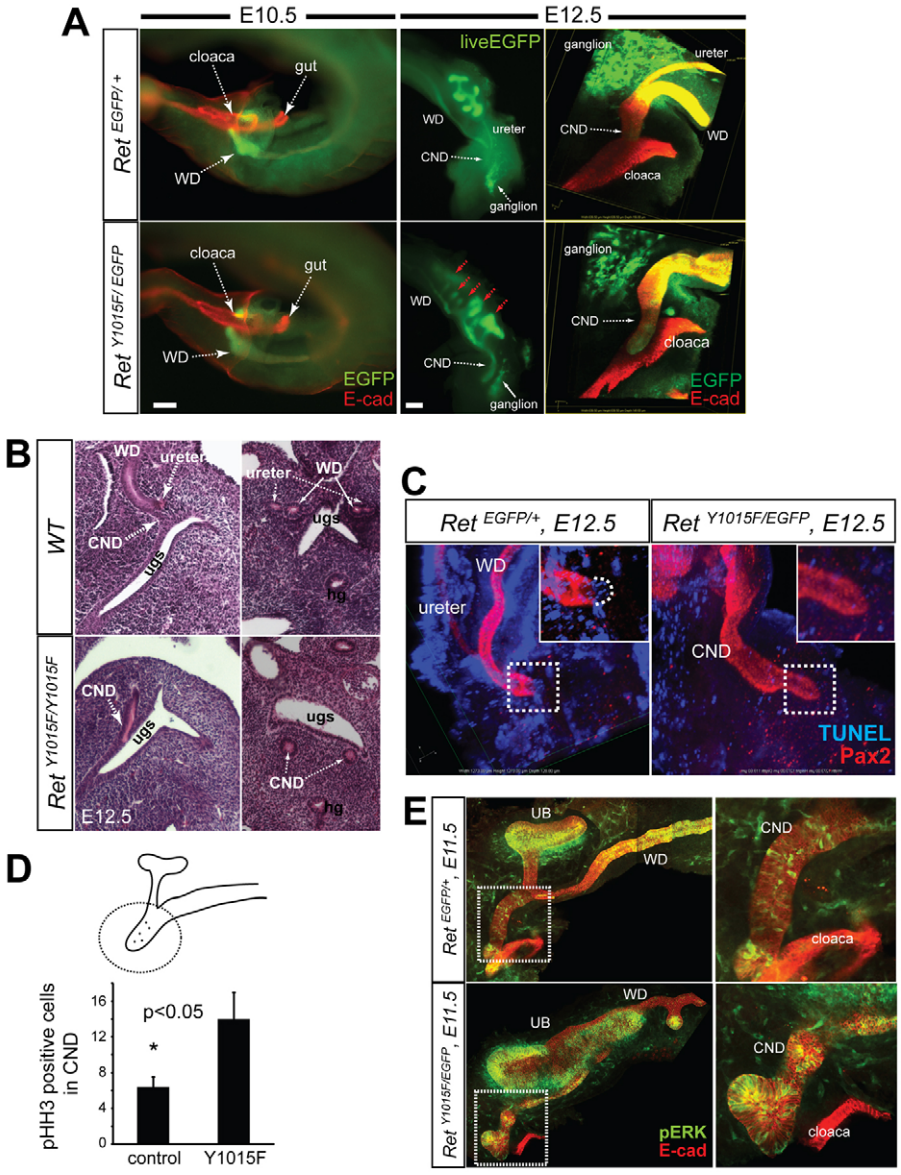

Fig. 6. Defects in CND degeneration in *RetY1015F* mutant mice. (**A**) Left, visualization of E-cadherin immunostaining and live EGFP signal from *Ret* locus at E10.5 shows that *RetY1015F* WDs reach cloaca as in controls. Middle, strong EGFP expression in distal WD in mutant $Ret^{Y1015F/EGFP}$ UT at E12.5 indicates persistent common nephric duct (CND) compared with its absence in controls ($Ret^{EGFP/+}$). Right, 3D-reconstructed confocal images of EGFP (green) and E-cadherin (red) immunohistochemistry shows that, in the controls, WD and ureter have separated, consistent with loss of Ret-EGFP expression in CND, and ureters are inserted into cloaca wall. *RetY1015F* mutants show EGFP positivity in distal CND that is not connected to cloaca. Scale bars: 200 μm. (**B**) Left, representative HE-stained sagittal sections from a series of E12.5 lower tract illustrate a distinct CND extending along the cloacal wall in *RetY1015F* mutants, whereas in wild type it is barely detectable. Right, transverse HE sections illustrate no WD-ureter separation in the mutants as only a single CND lumen is seen on each side of the urogenital sinus whereas distinct WD and ureter lumens are present in wild type. UGS, urogenital sinus; hg, hindgut. (**C**) Whole-mount confocal imaging of Pax2 (red) and TUNEL (blue) staining shows lack of apoptosis in the mutant ($Ret^{Y1015F/EGFP}$) CND (inset, higher magnification). Control ($Ret^{EGFP/+}$) shows normal apoptosis, as indicated by TUNEL-positive cells (dashed curved line in the inset). (**D**) Quantification of phospho-histone H3-positive cells in CND at E11.5 measured by 3D-reconstructed confocal images. Note increased proliferation in *RetY1015F* mutant CNDs (n=3, mean±s.d., *P<0.05, t-test). (**E**) Whole-mount immunohistochemistry and confocal imaging of E-cadherin (red) and phospho-ERK (pERK, green) shows increased pERK labeling in *RetY1015F* mutant CNDs (images on the right are higher magnification of the boxed areas).

the WD (Fig. 8). Failure to provide this trans-repression in *RetY1015F* mutant mice disrupts anteroposterior patterning, resulting in prolonged exposure of WD to GDNF in the persistent MesM that is now positioned adjacent to the WD. This sets a precedent for strong tropic signal for ectopic budding via increased ERK that provides trophic support to the caudal WD budding domain. Gdnf misexpression is probably due to sustained Pax2 (Brophy et al., 2001) expression in the mutant MesM. Sustained Pax2 expression is most probably due to failure of MesM to regress in a timely manner. The time-lapse images clearly show that one consequence of this is fusion of the caudal ectopic buds with the growing metanephros leading to multiple ureters, branching defects

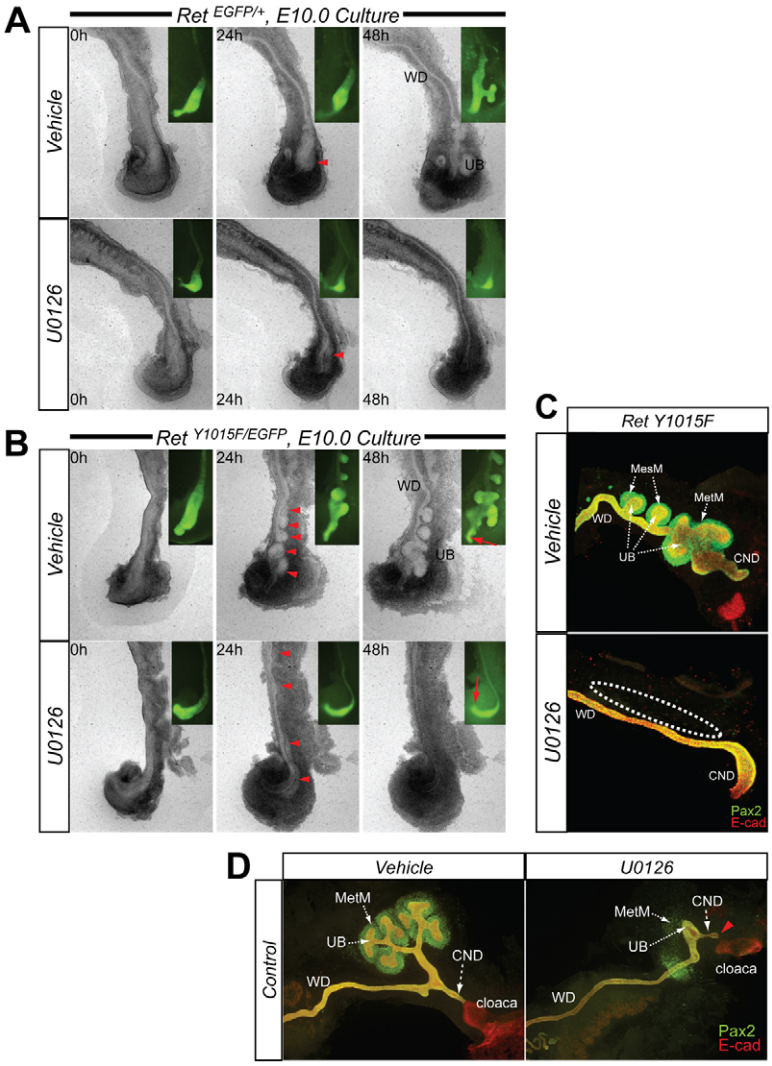

Fig. 7. Treatment with a MEK inhibitor attenuates ectopic budding and distal WD expansion in *RetY1015F* mutant UT explant cultures. (**A**,**B**) Phase-contrast time-lapse images at indicated timepoints of control (A, *Ret*$^{EGFP/+}$) and mutant (B, *Ret*$^{Y1015F/EGFP}$) UTs, beginning at E10 with vehicle (top row) or MEK inhibitor U0126 (10 μM, bottom row). In controls, U0126 treatment attenuates budding from distal WD. In mutants, multiple ectopic buds and distal expansion of WDs is inhibited in presence of U0126, indicating increased ERK signaling as a mechanism of these WD defects. Insets are live EGFP images clearly depicting the WD and budding regions. Red arrowheads at 24 hours, mesenchyme; red arrows at 48 hours in insets in B, distal WD/CND. (**C**) Double immunostaining of mutant UT cultures (48 hours) with Pax2 (green) and E-cad (red) show no Pax2 expression (outlined) in the mesenchyme in the mutants treated with U0126 compared with vehicle-treated cultures. This suggests that normal mesonephric domain is established by inhibiting MAPK activity in the mutants. (**D**) Double immunostaining of E11 control UT cultures (48 hours) with Pax2 (green) and E-cad (red) grown in presence of U0126 show common nephric duct (CND) aplasia (red arrowhead). The vehicle-treated CNDs are normally connected to the cloaca.

and multiplexed dysplastic kidneys. Inhibiting MAPK with a specific inhibitor attenuated growth of ectopic buds and CND aplasia in Y1015F mutants, further supporting that RetY1015F defects are at least mediated through MAPK. Whether increased ERK activity is also necessary for abnormal positioning of the mesenchyme or if increased ERK activity per cell is the cause of CND defects requires further investigation.

Slit2, *Robo2*, *Bmp4*, *Spry1* and *Gata3* knockout mice exhibit supernumerary UBs (Basson et al., 2005; Grieshammer et al., 2004; Grote et al., 2008; Miyazaki et al., 2000). Among these, *Robo2*- and *Slit2*-null mice (Grieshammer et al., 2004) show GU defects highly similar to *RetY1015F* mice, including mega-ureters, ectopic buds and cryptorchidism. In *Slit2*-null mice, ectopic UBs are due to extraneous *Gdnf* expression activating Ret only in the very caudal MesM. Because we did not see loss of *Slit2* expression in *RetY1015F* or malpositioning of Mes/MetM in *Slit2*-null WDs, we propose that RetY1015 and Slit2 regulate mesonephros development through different mechanisms. Spry1 is a negative regulator of MAPK and the ectopic buds in *Spry1*-null mice are thought to be due to increased MAPK activity in WD (Fisher et al., 2001). Reduced Ret activity in *Spry1* nulls normalizes ectopic buds (Rozen et al., 2009). Although Ret and Spry1 pathways appear to converge at the level of MAPK, it is not clear whether Ret directly modulates Spry1. Our expression analysis did not reveal loss of Spry1 in *Ret1015F* mutant WDs, suggesting that loss of Spry1 is not the mechanism of increased ERK activity and ectopic budding in these mutants. However, we cannot rule out the possibility that RetY1015 signals modulate Spry1 activity at a post-translational level.

Another novel discovery and insight from our studies is that RetY1015 regulates ureter-bladder union through a novel mechanism not intuitive from studies of *Ret*-null mice. Previous studies with null mice have demonstrated that retinoic acid-mediated Ret expression controls distal WD growth and CND degeneration (Batourina et al., 2002; Chia et al., 2011). Our analysis interestingly revealed that RetY1015 signals are important in the process of timely degeneration of the CND, beginning around E12.5. Persistence of the CND in *RetY1015F* mutant mice causes failure of ureter-WD separation and ureter defects. As in the upper tract, in the lower tract optimal ERK signaling appears to be a key process. Delayed degeneration in *RetY1015F* WDs is probably due to increased ERK activity causing increased proliferation and survival. Therefore, RetY1015-specific signals regulate WD/ureter connection to the bladder (including the ability to insert into cloaca) and CND remodeling, and encompass a spectrum of CND abnormalities that later translate into lower ureter abnormalities causing reflux and obstruction.

Mice deficient in *RPTP-LAR* (*Ptprf* and *Ptprs* – Mouse Genome Informatics) and *RetY1015* signaling exhibit similar ureter anomalies, suggesting they play a role in ureter remodeling through common

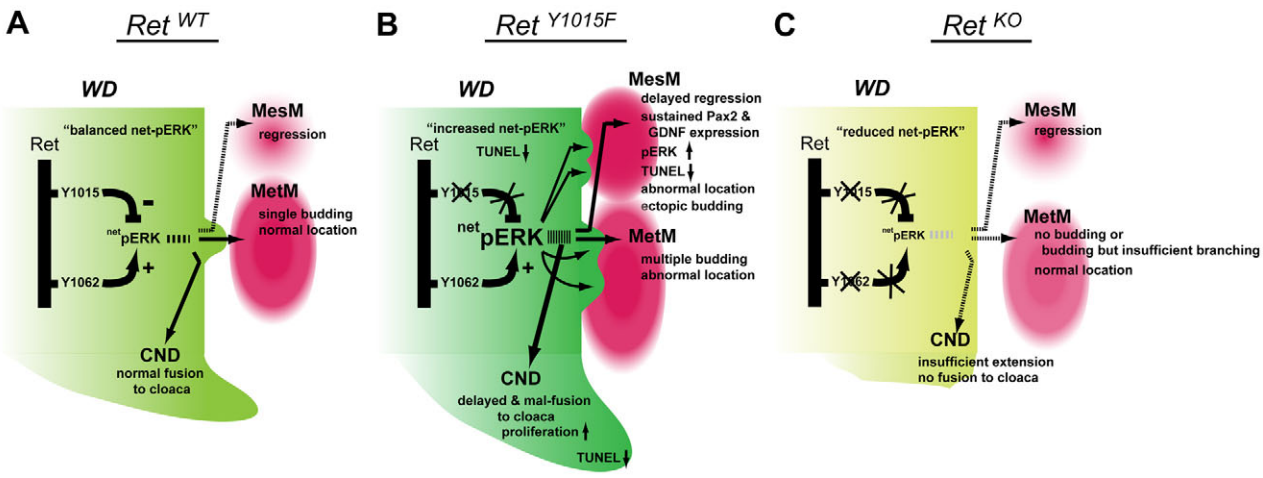

Fig. 8. Proposed model depicting molecular and developmental mechanisms of early urinary tract patterning through inhibitory roles of the RetY1015 docking site. (**A**) In normal urinary tracts (Ret^{WT}), net ERK signaling is optimally balanced by RetY1015 and RetY1062 docking sites to ensure MesM regression, normal mesenchyme position, single UB, and timely common nephric duct (CND) degeneration and fusion to cloaca. (**B**) Abrogation of RetY1015 signals (RetY1015F) results in increased ERK activity (represented by the larger font), reduced apoptosis, malpositioning of MesM and MetM, and delayed regression of MesM and CND. This results in ectopic UBs through sustained mesenchymal GDNF expression, branching defects and ureter-bladder junction abnormalities. (**C**) Loss of Ret abrogates all Ret-dependent signal transduction and results in reduced ERK activity (represented by the smaller font). This causes defects in distal WD elongation that results in a failure to fuse with the cloaca and UB induction that leads to agenesis. Thus, balance between inhibitory Ret signaling pathways regulated by RetY1015 and activating signals through other docking sites during early urinary tract development in amniotes is necessary to ensure that optimal ERK activity is maintained and that single kidney and ureter-bladder connections are established.

mechanisms (Basson et al., 2005; Jain et al., 2006a; Uetani et al., 2009). Uetani et al. reported that RPTP-LAR is a pro-apoptotic factor, as its deficiency results in increased CND survival due to reduced apoptosis (Uetani et al., 2009). Furthermore, these authors demonstrated that RPTP-LAR phosphatases normally inhibit pan-Ret signaling, as loss of RPTP-LAR results in hyperphosphorylation of RetY1015 and Y1062, implying that increased Ret activity promotes distal CND survival. Our studies suggest that RetY1015 activation in CND has a pro-apoptotic role. How does both activation (Uetani et al., 2009) and loss (our study) of Y1015 phosphorylation contribute to CND survival? One explanation is regulation of a common downstream compensatory/survival pathway, such as MAPK, that may be directly or indirectly modulated by RetY1015 (our study) and RPTP-LAR signaling (by regulating phosphorylation of RetY1015 and Y1062). Taken together, these analyses suggest that activating and inhibitory mechanisms modulate Ret-mediated ureter modeling that are Ret-extrinsic (RPTP-LAR) and Ret-intrinsic (Y1015) and at least affect the MAPK pathway.

Our current analyses using Ret signaling mutants as a paradigm provides insights and conceptual understanding of CAKUT pathogenesis even before branching morphogenesis begins. Specifically, our results demonstrate how Ret sculpts urinary system development through inhibitory roles of Y1015 docking tyrosine and maintains relationships between the urinary tract primordia and surrounding structures. The insights gleaned have direct relevance to human CAKUT pathogenesis owing to remarkable similarity between development of the rodent and human urinary system and Ret biology. In this regard, extremely deleterious mutations such as *RetY1062F* and *RetY1015F* are incompatible with life. However, mutations with milder effects on these pathways have less severe CAKUT, as illustrated by Gdnf-RetY1015F and Spry1-RetY1062F (Basson et al., 2005; Rozen et al., 2009) compound het-homozygous mutants. This supports the view that milder or severe mutations of genes in related pathways, when present together, can alter the outcomes of CAKUT. Importantly, these results demonstrate the need to develop efficient methods to diagnose CAKUT before metanephric kidney development and to indicate the types of cellular or developmental processes that can be targeted for clinical intervention.

Acknowledgements
We thank Angela Lluka and Amanda Knoten for excellent technical assistance.

Funding
This work was supported by National Institutes of Health (NIH) George M. O'Brien Center for Kidney Disease Research [P30-DK079333] to Washington University, by Children Discovery Institute [MDII2009177 to S.J.], and by the NIH [DK081644 and DK082531 to S.J.]. Deposited in PMC for release after 12 months.

Competing interests statement
The authors declare no competing financial interests.

Supplementary material
Supplementary material available online at
http://dev.biologists.org/lookup/suppl/doi:10.1242/dev.078667/-/DC1

References

Amiel, J. and Lyonnet, S. (2001). Hirschsprung disease, associated syndromes, and genetics: a review. *J. Med. Genet.* **38**, 729-739.
Amiel, J., Sproat-Emison, E., Garcia-Barcelo, M., Lantieri, F., Burzynski, G., Borrego, S., Pelet, A., Arnold, S., Miao, X., Griseri, P. et al. (2008). Hirschsprung disease, associated syndromes and genetics: a review. *J. Med. Genet.* **45**, 1-14.
Basson, M. A., Akbulut, S., Watson-Johnson, J., Simon, R., Carroll, T. J., Shakya, R., Gross, I., Martin, G. R., Lufkin, T., McMahon, A. P. et al. (2005). Sprouty1 is a critical regulator of GDNF/RET-mediated kidney induction. *Dev. Cell* **8**, 229-239.
Batourina, E., Choi, C., Paragas, N., Bello, N., Hensle, T., Costantini, F. D., Schuchardt, A., Bacallao, R. L. and Mendelsohn, C. L. (2002). Distal ureter morphogenesis depends on epithelial cell remodeling mediated by vitamin A and Ret. *Nat. Genet.* **32**, 109-115.
Batourina, E., Tsai, S., Lambert, S., Sprenkle, P., Viana, R., Dutta, S., Hensle, T., Wang, F., Niederreither, K., McMahon, A. P. et al. (2005). Apoptosis induced by vitamin A signaling is crucial for connecting the ureters to the bladder. *Nat. Genet.* **37**, 1082-1089.

Brophy, P. D., Ostrom, L., Lang, K. M. and Dressler, G. R. (2001). Regulation of ureteric bud outgrowth by Pax2-dependent activation of the glial derived neurotrophic factor gene. *Development* **128**, 4747-4756.
Chia, I., Grote, D., Marcotte, M., Batourina, E., Mendelsohn, C. and Bouchard, M. (2011). Nephric duct insertion is a crucial step in urinary tract maturation that is regulated by a *Gata3-Raldh2-Ret* molecular network in mice. *Development* **138**, 2089-2097.
Dressler, G. R. (2006). The cellular basis of kidney development. *Ann. Rev. Cell Dev. Biol.* **22**, 509-529.
Enomoto, H., Araki, T., Jackman, A., Heuckeroth, R. O., Snider, W. D., Johnson, E. M., Jr and Milbrandt, J. (1998). GFR α1-deficient mice have deficits in the enteric nervous system and kidneys. *Neuron* **21**, 317-324.
Fisher, C. E., Michael, L., Barnett, M. W. and Davies, J. A. (2001). Erk MAP kinase regulates branching morphogenesis in the developing mouse kidney. *Development* **128**, 4329-4338.
Grieshammer, U., Le M., Plump, A. S., Wang, F., Tessier-Lavigne, M. and Martin, G. R. (2004). SLIT2-mediated ROBO2 signaling restricts kidney induction to a single site. *Dev. Cell* **6**, 709-717.
Grote, D., Boualia, S. K., Souabni, A., Merkel, C., Chi, X., Costantini, F., Carroll, T. and Bouchard, M. (2008). Gata3 acts downstream of beta-catenin signaling to prevent ectopic metanephric kidney induction. *PLoS Genet.* 4, e1000316.
Jain, S. (2009). The many faces of RET dysfunction in kidney. *Organogenesis* **5**, 1-14.
Jain, S., Naughton, C. K., Yang, M., Strickland, A., Vij, K., Encinas, M., Golden, J., Heuckeroth, R., Johnson, E. and Milbrandt, J. (2004). Mice expressing a dominant-negative Ret mutation phenocopy human Hirschsprung disease and delineate a direct role of Ret in spermatogenesis. *Development* **131**, 5503-5513.
Jain, S., Encinas, M., Johnson, E. M., Jr and Milbrandt, J. (2006a). Critical and distinct roles for key RET tyrosine docking sites in renal development. *Genes Dev.* **20**, 321-333.
Jain, S., Golden, J. P., Wozniak, D., Pehek, E., Johnson, E. M., Jr and Milbrandt, J. (2006b). RET is dispensable for maintenance of midbrain dopaminergic neurons in adult mice. *J. Neurosci.* **26**, 11230-11238.
Jain, S., Knoten, A., Hoshi, M., Wang, H., Vohra, B. P., Heuckeroth, R. O. and Milbrandt, J. (2010). Organotypic specificity of RET-docking tyrosine residues in pathogenesis of neurocristopathies and renal malformations. *J. Clin. Invest.* **120**, 778-790.
Jijiwa, M., Fukuda, T., Kawai, K., Nakamura, A., Kurokawa, K., Murakumo, Y., Ichihara, M. and Takahashi, M. (2004). A targeting mutation of tyrosine 1062 in Ret causes a marked decrease of enteric neurons and renal hypoplasia. *Mol. Cell. Biol.* **24**, 8026-8036.
Kim, H. J. and Bar-Sagi, D. (2004). Modulation of signalling by Sprouty: a developing story. *Nat. Rev. Mol. Cell Biol.* **5**, 441-450.
Maeshima, A., Sakurai, H., Choi, Y., Kitamura, S., Vaughn, D. A., Tee, J. B. and Nigam, S. K. (2007). Glial cell derived neurotrophic factor independent ureteric bud outgrowth from the Wolffian duct. *J. Am. Soc. Nephrol.* **18**, 3147-3155.
Michos, O., Cebrian, C., Hyink, D., Grieshammer, U., Williams, L., D'Agati, V., Licht, J. D., Martin, G. R. and Costantini, F. (2010). Kidney development in the absence of Gdnf and Spry1 requires Fgf10. *PLoS Genet.* **6**, e1000809.
Miyazaki, Y., Oshima, K., Fogo, A., Hogan, B. L. and Ichikawa, I. (2000). Bone morphogenetic protein 4 regulates the budding site and elongation of the mouse ureter. *J. Clin. Invest.* **105**, 863-873.
Moore, M. W., Klein, R. D., Farinas, I., Sauer, H., Armanini, M., Phillips, H., Reichart, L. F., Ryan, A. M., Carver-Moore, K. and Rosenthal, A. (1996). Renal and neuronal abnormalities in mice lacking GDNF. *Nature* **382**, 76-79.
Moore, S. W. (2006). The contribution of associated congenital anomalies in understanding Hirschsprung's disease. *Pediatr. Surg. Int.* **22**, 305-315.
Murawski, I. J. and Gupta, I. R. (2008). Gene discovery and vesicoureteric reflux. *Pediatr. Nephrol.* **23**, 1021-1027.
Ponder, B. A. and Smith, D. (1996). The MEN II syndromes and the role of the ret proto-oncogene. *Adv. Cancer Res.* **70**, 179-222.
Pope, J. C., 4th, Brock, J. W., 3rd, Adams, M. C., Stephens, F. D. and Ichikawa, I. (1999). How they begin and how they end: classic and new theories for the development and deterioration of congenital anomalies of the kidney and urinary tract, CAKUT. *J. Am. Soc. Nephrol.* **10**, 2018-2028.
Prato, A. P., Musso, M., Ceccherini, I., Mattioli, G., Giunta, C., Ghiggeri, G. M. and Jasonni, V. (2009). Hirschsprung disease and congenital anomalies of the kidney and urinary tract (CAKUT): a novel syndromic association. *Medicine* **88**, 83-90.
Rogers, S. A., Ryan, G. and Hammerman, M. R. (1991). Insulin-like growth factors I and II are produced in the metanephros and are required for growth and development in vitro. *J. Cell Biol.* **113**, 1447-1453.
Rozen, E. J., Schmidt, H., Dolcet, X., Basson, M. A., Jain, S. and Encinas, M. (2009). Loss of Sprouty1 rescues renal agenesis caused by Ret mutation. *J. Am. Soc. Nephrol.* **20**, 255-259.
Sainio, K., Suvanto, P., Saarma, M., Arumœe, U., Lindahl, M., Davies, J. A. and Sariola, H. (1997). Glial Cell-line derived neurotrophic factor is a morphogen for the ureteric bud epithelium. *Development* **20**, 4077-4087.
Saxen, L. (1987). *Organogenesis of the Kidney*. Cambridge, UK: Cambridge University Press.
Schuchardt, A., D'Agati, V., Larsson-Blomberg, L., Costantini, F. and Pachnis, V. (1994). Defects in the kidney and enteric nervous system of mice lacking the tyrosine kinase receptor Ret. *Nature* **367**, 380-383.
Sebolt-Leopold, J. S. and Herrera, R. (2004). Targeting the mitogen-activated protein kinase cascade to treat cancer. *Nat. Rev. Cancer* **4**, 937-947.
Shakya, R., Jho, E. H., Kotka, P., Wu, Z., Kholodilov, N., Burke, R., D'Agati, V. and Costantini, F. (2005). The role of GDNF in patterning the excretory system. *Dev. Biol.* **283**, 70-84.
Skinner, M. A., Safford, S. D., Reeves, J. G., Jackson, M. E. and Freemerman, A. J. (2008). Renal aplasia in humans is associated with RET mutations. *Am. J. Hum. Genet.* **82**, 344.
Smith, C. and Mackay, S. (1991). Morphological development and fate of the mouse mesonephros. *J. Anat.* **174**, 171-184.
Uetani, N., Bertozzi, K., Chagnon, M. J., Hendriks, W., Tremblay, M. L. and Bouchard, M. (2009). Maturation of ureter-bladder connection in mice is controlled by LAR family receptor protein tyrosine phosphatases. *J. Clin. Invest.* **119**, 924-935.
Vainio, S. and Muller, U. (1997). Inductive tissue interactions, cell signaling, and the control of kidney organogenesis. *Cell* **90**, 975-978.
Wong, A., Bogni, S., Kotka, P., de Graaff, E., D'Agati, V., Costantini, F. and Pachnis, V. (2005). Phosphotyrosine 1062 is critical for the in vivo activity of the Ret9 receptor tyrosine kinase isoform. *Mol. Cell. Biol.* **25**, 9661-9673.